Discovering physical concepts with neural networks

Raban Iten[1 2], Tony Metger[1 2], Henrik Wilming[1], Lídia del Rio[1], and Renato Renner[1]

[1]Institute for Theoretical Physics, ETH Zürich, 8093 Zürich, Switzerland

[2]These authors contributed equally to this work.

The formalism of quantum physics is built upon that of classical mechanics. In principle, considering only experimental data without prior knowledge could lead to an alternative quantum formalism without conceptual issues like the measurement problem. As a first step towards finding such an alternative, we introduce a neural network architecture that models the physical reasoning process and can be used to extract simple physical concepts from experimental data in an unbiased way. For a variety of simple systems in classical and quantum mechanics, our network learns to compress experimental data to a simple representation and uses the representation to answer questions about the physical system. Physical concepts can be extracted from the learned representation: **(1)** The representation stores the physically relevant parameters, like the frequency of a pendulum. **(2)** The network finds and exploits conservation laws: it stores the total angular momentum to predict the motion of two colliding particles. **(3)** Given measurement data of a simple quantum mechanical system, the network correctly recognizes the number of degrees of freedom describing the underlying quantum state. **(4)** Given a time series of the positions of the Sun and Mars as observed from Earth, the network discovers the heliocentric model of the solar system — that is, it encodes the data into the angles of the two planets as seen from the Sun.

1 Introduction

Theoretical physics, like all fields of human activity, is influenced by the schools of thought prevalent at the time of development. As such, the physical theories we know may not necessarily be the simplest ones to explain the experimental data, but rather the ones that most naturally followed from a previous theory at the time. The formalism of quantum theory, for instance, is built upon classical mechanics; it has been impressively successful, but leads to conceptually challenging consequences (see [1, 2] for a review and [3] for a recent example).

This raises an interesting question: are the laws of quantum physics, and other physical theories more generally, the most natural ones to explain data from experiments if we assume no prior knowledge of physics? While this question will likely not be answered fully in the near future, recent advances in artificial intelligence allow us to make a first step in this direction. Here, we investigate whether neural networks can be used to discover physical concepts in classical and quantum mechanics from experimental data, without imposing prior assumptions and restrictions on the space of possible concepts.

While neural networks have been applied to a variety of problems in physics, most work to date has focused on the efficiency or quality of predictions of neural networks, without an understanding of what the network learned [4–10] (see Section 4.1 for a comparison with previous work). Other algorithms and neural network architectures have been developed to produce a physical model by imposing some structure on the space of solutions and on the input data [11–13]. For example, in [11], an algorithm recovers the laws of motion of simple mechanical systems like a double pendulum. The search for physical laws is done over a space of mathematical expressions on the input variables. To apply this method, we

Raban Iten: itenr@itp.phys.ethz.ch

Tony Metger: tmetger@ethz.ch

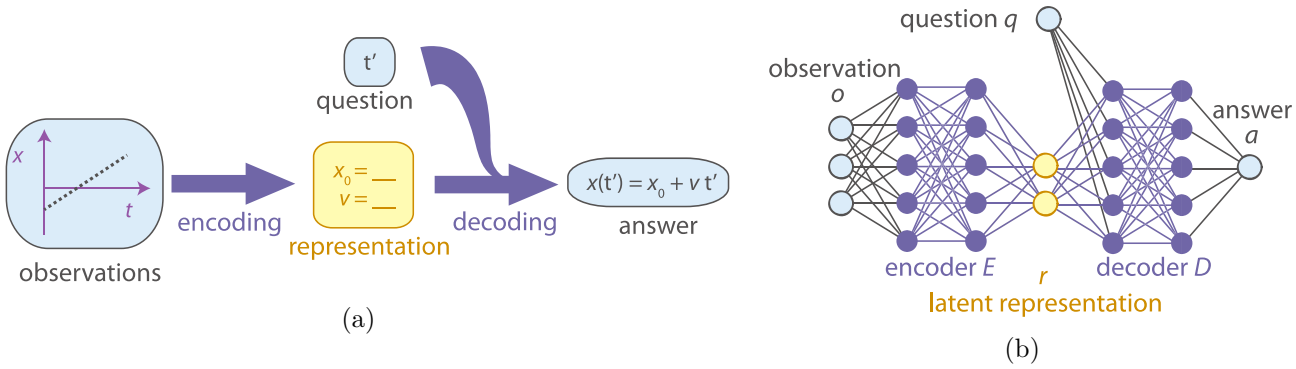

Figure 1: **Representation learning of physical concepts. (a) Human learning.** A physicist compresses experimental observations into a simple representation (*encoding*). When later asked any question about the physical setting, the physicist should be able to produce a correct answer using only the representation and not the original data — in this case we say that the representation is *sufficient* for the problem. The process of producing the answer (by applying a physical model to the representation) is called *decoding*. For example, the observations may be the first few seconds of the trajectory of a particle moving with constant speed; the representation could be the parameters "speed v" and "initial position x_0" and the question could be "where will the particle be at a later time t'?" The decoder implements the appropriate equation of motion using the information in the representation in order to produce an answer. **(b) Neural network structure for *SciNet*.** Observations are encoded as real parameters fed to an encoder (a *feed-forward neural network*, see Appendix A), which compresses the data into a representation (*latent representation*). The question is again encoded in a number of real parameters, which, together with the representation, are fed to the decoder network to produce an answer. Note that the number of layers and neurons depicted is just an example, and not representative.

must specify *a priori* which variables may enter the mathematical models, and how they can be combined; in other words, we must impose on the network our intuition of which parameters will be physically relevant. Here, however, we are interested in questioning those same intuitions, and asking whether an unconstrained neural network would characterize physical settings through parameters and representations similar to those of standard physics textbooks.

1.1 Network structure: *SciNet*

To approach this task, we apply supervised and unsupervised machine learning techniques using ideas from representation learning [14–19]. Concretely, we introduce a neural network architecture, which we call *SciNet* for brevity, which mimics a physicist's modelling process (Figure 1a), and apply it to study various physical scenarios. The idea is that the physicist (or *SciNet*) is exposed to some experimental observations pertaining to a physical setting (e.g. a time series $(t_i, x(t_i))_{i\in\{1,\dots,N\}}$ describing the movement of a particle at constant speed), finds a simpler representation (e.g. the two parameters initial position and speed, $(x(t_0), v)$), and will later be asked a question about this physical setting (e.g. "where is the particle at time t'?"). Ideally, the representation should be as compact as possible while still fully characterizing the physics of the situation, so that the physicist may forget the original data and answer the question using only the representation (Section 3).

For a purely input-output (black box) analysis, the modelling process of *SciNet* can be seen as a map $F : \mathcal{O} \times \mathcal{Q} \to \mathcal{A}$ from the sets of possible observations $\mathcal{O}$ and questions $\mathcal{Q}$ to the set of possible answers $\mathcal{A}$. We can split this map into an *encoder* $E : \mathcal{O} \to \mathcal{R}$ mapping the original observation to a compressed representation (called *latent representation* in machine learning), followed by a *decoder* $D : \mathcal{R} \times \mathcal{Q} \to \mathcal{A}$ that takes the representation and the question to produce an answer. The corresponding network structure is shown in Figure 1b. A similar network architecture was recently applied for scene representation and rendering [20]. It is this decomposition, $F(o, q) = D(E(o), q)$, that will allow us to implement the encoder and decoder as a neural network in such a way that we can interpret the network's learned representation, by analyzing how it changes as we tweak known parameters of the setting. In order to force

Box 1: Time evolution of a damped pendulum (Section 2.1)

Problem: Predict the position of a one-dimensional damped pendulum at different times.

Physical model: Equation of motion: $m\ddot{x} = -\kappa x - b\dot{x}$.
Solution: $x(t) = A_0 e^{-\frac{b}{2m}t}\cos(\omega t + \delta_0)$, with $\omega = \sqrt{\frac{\kappa}{m}}\sqrt{1 - \frac{b^2}{4m\kappa}}$.

Observation: Time series of positions: $o = \big[x(t_i)\big]_{i\in\{1,\ldots,50\}} \in \mathbb{R}^{50}$, with equally spaced t_i. Mass $m = 1$kg, amplitude $A_0 = 1$m and phase $\delta_0 = 0$ are fixed; spring constant $\kappa \in [5, 10]$ kg/s^2 and damping factor $b \in [0.5, 1]$ kg/s are varied between training samples.

Question: Prediction times: $q = t_{\text{pred}} \in \mathbb{R}$.

Correct answer: Position at time t_{pred}: $a_{\text{cor}} = x(t_{\text{pred}}) \in \mathbb{R}$.

Implementation: Network depicted in Figure 1b with 3 latent neurons.

Key findings:

- *SciNet* predicts the positions $x(t_{\text{pred}})$ with a root mean square error below 2% (with respect to the amplitude $A_0 = 1$m) (Figure 2a).
- *SciNet* stores κ and b in two of the latent neurons, and does not store any information in the third latent neuron (Figure 2b).

SciNet to find and exploit the physical structure of a problem, we motivate it to minimize the number of neurons in the latent representation (see Section 2 for examples and Section 3 for theoretical considerations). We use fully connected feed-forward neural networks to implement the encoder and the decoder of *SciNet* (see Appendix A for an introduction to neural networks).

1.2 Training and testing *SciNet*

We train *SciNet* with data samples of the form $(o, q, a_{\text{cor}}(o, q))$, where the observation o and question q are chosen from the sets $\mathcal{O}$ and $\mathcal{Q}$ of all possible observations and questions, respectively, and where $a_{\text{cor}}(o, q)$ denotes the correct reply to question q given observation o.

We consider families of encoders E_ϕ and decoders D_θ, parameterized by the weights and biases of the encoding and decoding networks, which we summarize into the parameter sets ϕ and θ, respectively. During training, we motivate *SciNet* to adapt its free parameters ϕ and θ to improve its prediction accuracy and to learn *minimal uncorrelated representations* (see Section 3, Appendix B). For this, we use methods from representation learning, specifically disentangling variational autoencoders [14, 18, 21, 22].

We do not impose which representation of the physical setting *SciNet* should learn; *SciNet* makes this choice in an unsupervised way, even though the correct answers are provided in a supervised way. In the special case where we always ask the same question, namely to reproduce the input, *SciNet* has the same structure as an autoencoder. In this case, the training is fully unsupervised.

To make good predictions, *SciNet* needs a sufficient number of latent neurons. Knowing nothing about the physical system under consideration, we might choose this number to be too small. In that case, *SciNet* will make predictions with low accuracy and we can set up a new network with more latent neurons. To determine the prediction accuracy, we test *SciNet* on new data samples (*test data*), which have not been seen during training.

Once the network is trained to make accurate predictions, our aim is to read out conceptual information from the representation it found. For any given observation, we consider the activations of the neurons in the latent representation (which are real numbers) as the values of the (unknown) physical variables present in the observation.

2 Results

We demonstrate with four examples how *SciNet* is able to recover the relevant physical variables, both in quantum and in classical systems. Moreover, we will show that *SciNet* can be used to recover important concepts of physics, like conserved quantities or the heliocentric model of our solar system. A theoretical analysis follows in Sec-

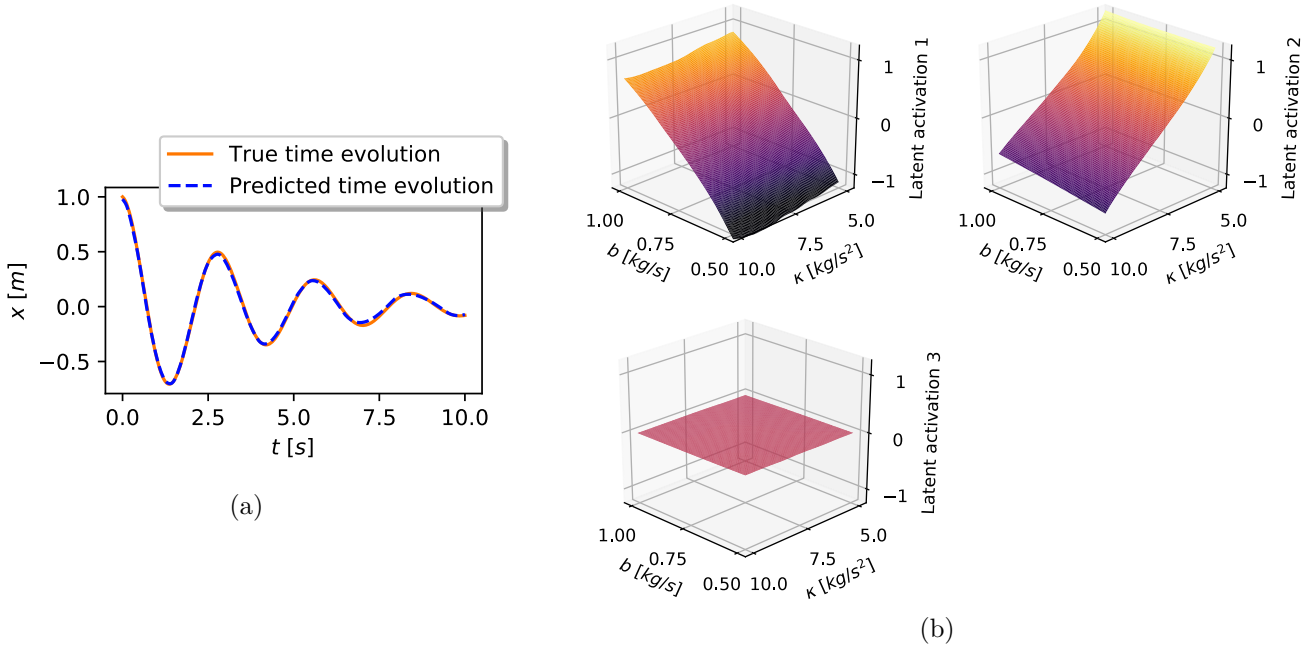

Figure 2: **Damped pendulum**. *SciNet* is fed a time series of the trajectory of a damped pendulum. It learns to store the two relevant physical parameters, frequency and damping, in the representation, and makes correct predictions about the pendulum's future position. **(a) Trajectory prediction of *SciNet*.** Here, spring constant $\kappa = 5\text{kg/s}^2$ and damping factor $b = 0.5\text{kg/s}$. *SciNet's* prediction is in excellent agreement with the true time evolution. **(b) Representation learned by *SciNet*.** The plots show the activations of the three latent neurons of *SciNet* as a function of the spring constant κ and the damping factor b. The first two neurons store the damping factor and spring constant, respectively. The activation of the third neuron is close to zero, suggesting that only two physical variables are required.

tion 3.

2.1 Damped pendulum

We start with a simple example from classical physics, the damped pendulum, described in Box 1. The time evolution of the system is described by the differential equation $-\kappa x - b\dot{x} = m\ddot{x}$, where κ is the *spring constant*, which determines the frequency of the oscillation, and b is the *damping factor*. We keep the mass m constant (it is a scaling factor that could be absorbed by defining $\kappa' = \kappa/m$ and $b' = b/m$), such that κ and b are the only variable parameters. We consider the case of weak damping here, where the solution to the equation of motion is given in Box 1.

We choose a network structure for *SciNet* with 3 latent neurons. The accuracy of the predictions given by *SciNet* after training is illustrated in Figure 2a.

Without being given any physical concepts, *SciNet* learns to extract the two relevant physical parameters from time series data for the x-coordinate of the pendulum and to store them in the latent representation. As shown in Figure 2b, the first latent neuron depends nearly linearly on b and is almost independent of κ, and the second latent neuron depends only on κ, again almost linearly. Hence, *SciNet* has recovered the same time-independent parameters b and κ that are used by physicists. The third latent neuron is nearly constant and does not provide any additional information — in other words, *SciNet* recognized that two parameters suffice to encode this situation.

2.2 Conservation of angular momentum

One of the most important concepts in physics is that of conservation laws, such as conservation of energy and angular momentum. While their relation to symmetries makes them interesting to physicists in their own right, conservation laws are also of practical importance. If two systems interact in a complex way, we can use conservation laws to predict the behaviour of one system from the behaviour of the other, without studying the details of their interaction. For certain types of questions, conserved quantities therefore act as a compressed representation of joint properties of several systems.

Box 2: Collision of two bodies under angular momentum conservation (Section 2.2)

Problem: Predict the position of a particle fixed on a rod (rotating about the origin) after a collision at a fixed point with a free particle (in two dimensions, see Figure 3a).

Physical model: Given the total angular momentum before the collision and the velocity of the free particle after the collision, the position of the rotating particle at time t'_{pred} (after the collision) can be calculated from angular momentum conservation: $J = m_{\text{rot}} r^2 \omega - r m_{\text{free}} (\mathbf{v}_{\text{free}})_x = m_{\text{rot}} r^2 \omega' - r m_{\text{free}} (\mathbf{v}'_{\text{free}})_x = J'$.

Observation:
Time series of both particles before the collision: $o = [(t_i^{\text{rot}}, \mathbf{q}_{\text{rot}}(t_i^{\text{rot}})), (t_i^{\text{free}}, \mathbf{q}_{\text{free}}(t_i^{\text{free}}))]_{i\in\{1,\ldots,5\}}$, with times t_i^{rot} and t_i^{free} randomly chosen for each training sample. Masses $m_{\text{rot}} = m_{\text{free}} = 1\text{kg}$ and the orbital radius $r = 1\text{m}$ are fixed; initial angular momentum ω, initial velocity $\mathbf{v}_{\text{free}}$ and final velocity $\mathbf{v}'_{\text{free}}$ are varied between training samples. Gaussian noise ($\mu = 0, \sigma = 0.01\text{m}$) is added to all position inputs.

Question: Prediction time and position of free particle after collision: $q = \left(t'_{\text{pred}}, [t'_i, \mathbf{q}'_{\text{free}}(t'_i)]_{i\in\{1,\ldots,5\}}\right)$.

Correct answer: Position of rotating particle at time t'_{pred}: $a_{\text{cor}} = \mathbf{q}'_{\text{rot}}(t'_{\text{pred}})$.

Implementation: Network depicted in Figure 1b with one latent neuron.

Key findings:

- *SciNet* predicts the position of the rotating particle with root mean square prediction error below 4% (with respect to the radius $r = 1\text{m}$).
- *SciNet* is resistant to noise.
- *SciNet* stores the total angular momentum in the latent neuron.

The following example shows that *SciNet* can recover angular momentum conservation from (simulated) experimental data. We consider the scattering experiment shown in Figure 3 and described in Box 2, where two point-like particles collide. Given the initial angular momentum of the two particles and the final trajectory of one of them, a physicist can predict the trajectory of the other using conservation of total angular momentum.

To see whether *SciNet* learns the same idea, we train it with (simulated) experimental data as described in Box 2 with one latent neuron, and add Gaussian noise to show that the encoding and decoding are robust. Indeed, *SciNet* does exactly what a physicist would do and stores the total angular momentum in the latent representation (Figure 3b). This example shows that *SciNet* can recover conservation laws, and suggests that they emerge naturally from compressing data and asking questions about joint properties of several systems.

2.3 Representation of qubits

In quantum mechanics, it is not trivial to construct a simple representation of the state of a quantum system from measurement data. Indeed, investigating which measurements are needed to fully specify a quantum state is an active area of research called *quantum state tomography* [23]. Ideally, we look for a *faithful representation* of the state of a quantum system, such as the wave function: a representation that stores all information necessary to predict the probabilities of obtaining different outcomes in arbitrary measurements on that system. If a set of measurements is sufficient to reconstruct the full quantum state, such a set is called *tomographically complete*.

Here we show that, based only on (simulated) experimental data and without being given any assumptions about quantum theory, *SciNet* recovers a faithful representation of the state of small quantum systems and can make accurate predictions. In particular, this allows us to infer the dimension of the system and distinguish tomographically complete from incomplete measurement sets. Box 3 summarizes the setting and the results.

In quantum mechanics, the simplest system is a qubit, the quantum-mechanical analogue to the classical bit. A (pure) state on n qubits can be represented by a normalized complex vector $\psi \in \mathbb{C}^{2^n}$, where two states ψ and ψ' are identified if

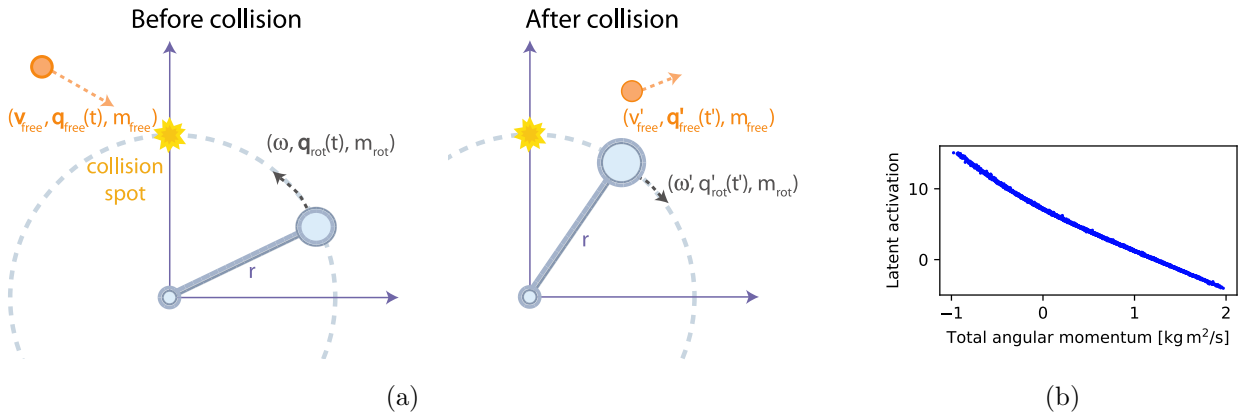

(a) (b)

Figure 3: **Collision under conservation of angular momentum.** In a classical mechanics scenario where the total angular momentum is conserved, the neural network learns to store this quantity in the latent representation. **(a) Physical setting.** A body of mass m_{rot} is fixed on a rod of length r (and of negligible mass) and rotates around the origin with angular velocity ω. A free particle with velocity $\mathbf{v}_{\text{free}}$ and mass m_{free} collides with the rotating body at position $\mathbf{q} = (0, r)$. After the collision, the angular velocity of the rotating particle is ω' and the free particle is deflected with velocity $\mathbf{v}'_{\text{free}}$. **(b) Representation learned by *SciNet*.** Activation of the latent neuron as a function on the total angular momentum. *SciNet* learns to store the total angular momentum, a conserved quantity of the system.

and only if they differ by a global phase factor, i.e., if there exist a $\phi \in \mathbb{R}$ such that $\psi = e^{i\phi}\psi'$. The normalization condition and irrelevance of the global phase factor decrease the number of free parameters of a quantum state by two. Since a complex number has two real parameters, a single-qubit state is described by $2 \times 2^1 - 2 = 2$ real parameters, and a state of two qubits is described by $2 \times 2^2 - 2 = 6$ real parameters.

Here, we consider binary projective measurements (with measurement outcomes labelled by 0 for the projection on ω and 1 otherwise) on n qubits. Just like states, the measurements that we consider can be described by vectors $\omega \in \mathbb{C}^{2^n}$. The probability to get outcome 0 measuring ω on a quantum system in the state ψ is then given by $p(\omega, \psi) = |\langle \omega, \psi \rangle|^2$, where $\langle \cdot, \cdot \rangle$ denotes the standard scalar product on $\mathbb{C}^{2^n}$.

To generate the training data for *SciNet*, we assume that we have one or two qubits in a lab that can be prepared in arbitrary states and we have the ability to perform binary projective measurements in a set $\mathcal{M}$. We choose n_1 measurements $\mathcal{M}_1 := \{\alpha_1, \ldots, \alpha_{n_1}\} \subset \mathcal{M}$ randomly, which we would like to use to determine the state of the quantum system. We perform all measurements in $\mathcal{M}_1$ several times on the same quantum state ψ to estimate the probabilities $p(\alpha_i, \psi)$ of measuring 0 for the i-th measurement. These probabilities form the observation given to *SciNet*.

To parameterize the measurement ω, we choose another random set of measurements $\mathcal{M}_2 := \{\beta_1, \ldots, \beta_{n_2}\} \subset \mathcal{M}$. The probabilities $p(\beta_i, \omega)$ specify the question for *SciNet*. We always assume that we have chosen enough measurements in $\mathcal{M}_2$ such that they can distinguish all the possible measurements $\omega \in \mathcal{M}$, i.e., we assume that $\mathcal{M}_2$ is tomographically complete.[1] *SciNet* then has to predict the probability $p(\omega, \psi)$ for measuring the outcome 0 on the state ψ when performing the measurement ω.

We train *SciNet* with different pairs (ω, ψ) for one and two qubits, keeping the measurement sets $\mathcal{M}_1$ and $\mathcal{M}_2$ fixed. We choose $n_1 = n_2 = 10$ for the single-qubit case and $n_1 = n_2 = 30$ for the two-qubit case. The results are shown in Figure 4.

Varying the number of latent neurons, we can observe how the quality of the predictions improves as we allow for more parameters in the representation of ψ. To minimize statistical fluctuations due to the randomized initialization of the network, each network specification is trained

[1] This parameterization of a measurement ω assumes that we know the equivalence between binary projective measurements and states. However, this is not a fundamental assumption, since we could parameterize the set of possible measurements by any parameterization that is natural for the experimental setup. Because $\mathcal{M}_2$ only represents a specific choice for parameterizing the measurement setup, it is natural to assume that $\mathcal{M}_2$ is tomographically complete.

Box 3: Representation of pure one- and two-qubit states (Section 2.3)

Problem: Predict the measurement probabilities for any binary projective measurement $\omega \in \mathbb{C}^{2^n}$ on a pure n-qubit state $\psi \in \mathbb{C}^{2^n}$ for $n = 1, 2$.

Physical model: The probability $p(\omega, \psi)$ to measure 0 on the state $\psi \in \mathbb{C}^{2^n}$ performing the measurement $\omega \in \mathbb{C}^{2^n}$ is given by $p(\omega, \psi) = |\langle \omega, \psi \rangle|^2$.

Observation: Parameterization of a state ψ: $o = [p(\alpha_i, \psi)]_{i \in \{1,\ldots,n_1\}}$ for a fixed set of random binary projective measurements $\mathcal{M}_1 := \{\alpha_1, \ldots, \alpha_{n_1}\}$ ($n_1 = 10$ for one qubit, $n_1 = 30$ for two qubits).

Question: Parameterization of a measurement ω: $q = [p(\beta_i, \omega)]_{i \in \{1,\ldots,n_2\}}$ for a fixed set of random binary projective measurements $\mathcal{M}_2 := \{\beta_1, \ldots, \beta_{n_2}\}$ ($n_2 = 10$ for one qubit, $n_2 = 30$ for two qubits).

Correct answer: $a_{\text{cor}}(\omega, \psi) = p(\omega, \psi) = |\langle \omega, \psi \rangle|^2$.

Implementation: Network depicted in Figure 1b with varying numbers of latent neurons.

Key findings:

- *SciNet* finds the minimal number of parameters necessary to describe the state ψ (see Figure 4).
- *SciNet* distinguishes tomographically complete and incomplete sets of measurements (see Figure 4).

three times and the run with the lowest mean square prediction error on the test data is used.

For the cases where $\mathcal{M}_1$ is tomographically complete, the plots in Figure 4 show a drop in prediction error when the number of latent neurons is increased up to two or six for the cases of one and two qubits, respectively. This is in accordance with the number of parameters required to describe a one or a two qubit state.

In the case of a single qubit there is an additional small (but significant) improvement in going from two to three latent neurons: this is caused by the fact that the two-parameter representation of a single qubit, for example the Bloch sphere representation, includes a *cyclic parameter*, which cannot be exactly represented by a continuous encoder (Appendix D). This restriction also makes it difficult to interpret the details of the learned representation.

SciNet can also be used to determine whether the measurement set $\mathcal{M}_1$ is tomographically complete or not. To generate tomographically incomplete data, we choose the measurements in $\mathcal{M}_1$ randomly from a subspace of all binary projective measurements. For a single qubit, we use a two-dimensional (real) subspace of measurements; for two quibts, we use a three-dimensional (real) subspace.

Given tomographically incomplete data about a state ψ, it is not possible for *SciNet* to predict the outcome of the final measurement perfectly regardless of the number of latent neurons, in contrast to the tomographically complete case (see Figure 4). Hence, we can deduce from *SciNet's* output (see Figure 4) that $\mathcal{M}_1$ is an incomplete set of measurements. Furthermore, the prediction error does not improve when using more than two latent neurons for the single qubit and more than three latent neurons for two qubits. This suggests that the measurement set $\mathcal{M}_1$ consists of two independent measurements for a single qubit and three independent measurements for two qubits, in accordance with the dimensions of the measurement subspaces we chose.[2]

2.4 Heliocentric model of the solar system

When observed from Earth, the orbits of the Sun and the other planets in our solar system take complicated shapes. In the 16th century, Copernicus measured the angles between a distant fixed star and several planets and celestial bodies (Figure 6a) and hypothesized that the Sun, and not the Earth, is in the centre of our solar system and that the planets move around the Sun on simple orbits. This explains the complicated orbits as seen from Earth.

Here, we show that *SciNet* similarly uses heliocentric angles when forced to find a representation for which the time evolution of the variables takes a very simple form, a typical requirement for time-dependent variables in physics.

[2] In contrast to the tomomgraphically complete case, all information given about a single qubit by two measurements can be encoded in two non-cyclic parameters, so the cyclicity problem from before does not arise here.

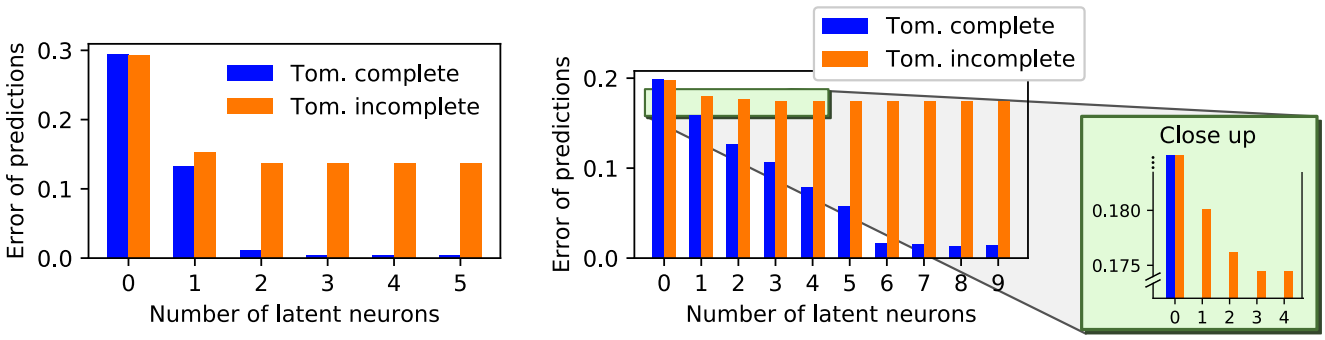

(a) One qubit. (b) Two qubits.

Figure 4: **Quantum tomography.** *SciNet* is given tomographic data for one or two qubits and has to predict the probabilities of outcomes of future measurements. We train *SciNet* with both tomographically complete and incomplete sets of measurements, and find that, given tomographically complete data, *SciNet* finds the minimal number of parameters needed to describe a quantum state (two parameters for one qubit and six parameters for two qubits). For tomographically incomplete data, *SciNet* cannot achieve perfect prediction accuracy. In this case, it finds our choice for the dimension of the subspace of (incomplete) measurements (two for one qubit and three for two qubits). The plots show the root mean square error of *SciNet's* measurement predictions for test data as a function of the number of latent neurons.

In the first three examples, we saw that *SciNet* is able to learn representations of time-independent parameters of different physical systems. In order to study the time evolution of the variables stored in the network's representation, we extend the network structure slightly (Figure 5).

Ideally we want the representation to store variables that evolve under simple rules — in this example, if *SciNet* stored the angles as seen from the Sun, the evolution would take a very simple form, whereas evolving the angles as seen from Earth requires the implementation of a much more involved time evolution. In order to find variables with a simple time evolution, we add a very small feed-forward neural network after the representation, which is meant to evolve the variables by a time step Δt. We can concatenate a series of identical time evolution networks and representation layers $\{r(t_i)\}_i$ to simulate step-wise evolution of the variables over a long period of time. We thus model the time evolution using a *recurrent neural network*.

After each step of the time evolution, we may again ask a question about the representation $r(t_i)$ — this is done by attaching a decoder D to the representation, as before. In this example we always ask the same question: "what are the angles as seen from Earth at the time t_i?" Hence, we do not need to feed a question as a new input to the decoder explicitly (but using an explicit question is in principle possible). The decoder at each time step is identical, and it receives the representation $r(t_i)$ as an input. The same representation $r(t_i)$ is also forwarded to the next time evolution step.

In this example, we restrict the latent layer to two neurons, and the time evolution network to maps of the simple form $r_j(t_i) \to r_j(t_i) + b_j$ on the j-th component $r_j(t_i)$ of the representation, where the biases b_j are the same for all time steps.[3] The setting is summarized in Box 4.

The activations of the two latent neurons of the trained network are plotted in Figure 6b. As can be seen from the plots, the activations of the latent representation are given by a linear combination of the angles ϕ_E and ϕ_M as seen from the Sun — *SciNet* has discovered the heliocentric model of the solar system. *SciNet* is not expected to store the angles ϕ_E and ϕ_M in separate neurons,

[3]For a general system, there might not exist a representation that admits such a simple time evolution. In this case, one has to proceed as follows: first, the time evolution is restricted to the simplest possible case, i.e., addition of a constant. If the network is unable to achieve good prediction accuracy, more complexity is added to the time evolution network until the network is able to make good predictions. Following this prescription, one will end up with the representation of the system that admits the simplest possible time evolution. However, for time evolution steps that are more complex than an affine function, it remains to be investigated how to quantify the complexity of the time evolution network in a meaningful way.

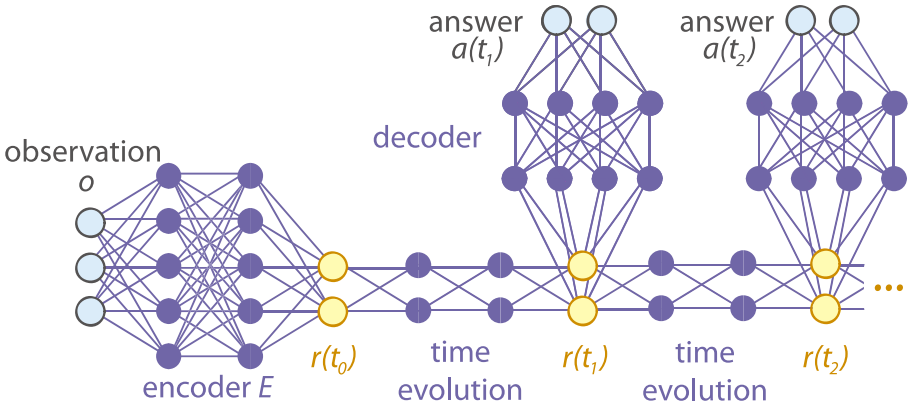

Figure 5: **Recurrent version of *SciNet* for time-dependent variables.** Observations are encoded into a simple representation $r(t_0)$ at time t_0. Then, the representation is evolved in time to $r(t_1)$ and a decoder is used to predict $a(t_1)$, etc. In each (equally spaced) time step, the same time evolution network and decoder network are applied.

since the time evolution update rule for any linear combination of the angles is still of the same simple form specified above.

3 Minimal representations

Here, we describe some of the theoretical considerations that went into designing *SciNet* and helping it to find useful representations that encode physical principles. Given a data set, it is generally a complex task to find a simple representation of the data that contains all the desired information. *SciNet* should recover such representations by itself; however, we motivate it to learn "simple" representations during training. To do so, we have to specify the desired properties of a representation. In this, our approach follows the spirit of several works on representation learning theory [14–19].

For the theoretical analysis, we introduce some additional structure on the data that is required to formulate the desired properties of a representation. We consider real-valued data, which we think of as being sampled from some unknown probability distribution. In other words, we consider random variables O, Q, R and A for the observations, the questions, the latent representations, and the answers, respectively, with samples lying in the sets $\mathcal{O} \subset \mathbb{R}^{|O|}, \mathcal{Q} \subset \mathbb{R}^{|Q|}, \mathcal{R} \subset \mathbb{R}^{|R|}$ and $\mathcal{A} \subset \mathbb{R}^{|A|}$, where $|X|$ denotes the number of real parameters of a random variable X (or, more formally, the dimension of the ambient space of the image of a random variable X).

The data is collected from observations on (simulated) physical systems over several runs. We assume that there exists a small number of hidden variables that fully describe the experimental data (similar models are used in representation learning, see for example [18]). These hidden variables are commonly called *hidden generative factors*. In each experimental run, we take a sample $g \in \mathcal{G} \subset \mathbb{R}^{|G|}$ of a small number $|G|$ of independent hidden generative factors, which are described by a random variable G. The high-dimensional measurement data is then "generated" by applying a map $H : \mathcal{G} \to \mathcal{O}$.

We require the following properties for an *uncorrelated (sufficient) representation* R (defined through an encoder mapping $E : \mathcal{O} \to \mathcal{R}$) for the data described by the triple (O, Q, a_{cor}), where the function $a_{\text{cor}} : \mathcal{O} \times \mathcal{Q} \to \mathcal{A}$ sends an observation $o \in \mathcal{O}$ and a question $q \in \mathcal{Q}$ to the correct answer $a \in \mathcal{A}$.

1. **Sufficient (with smooth decoder)**: There exists a smooth map[4] $D : \mathcal{R} \times \mathcal{Q} \mapsto \mathcal{A}$, such that $D(E(o), q) = a_{\text{cor}}(o, q)$ for all possible observations $o \in \mathcal{O}$ and questions $q \in \mathcal{Q}$.

2. **Uncorrelated**: The elements in the set $\{R_1, R_2, \ldots, R_{|R|}\}$ are mutually independent, where R_i denotes the i-th component of the representation R, interpreted as a random variable.

Property 1 asserts that the encoder map E encodes all information of the observation $o \in \mathcal{O}$ that is necessary to reply to all possible questions $q \in \mathcal{Q}$. We require the decoder to be smooth,

[4] It would be enough to require the decoder to be locally smooth for all the statements in this work.

Box 4: Heliocentric model of the solar system (Section 2.4)

Problem: Predict the angles $\theta_M(t)$ and $\theta_S(t)$ of Mars and the Sun as seen from Earth, given initial states $\theta_M(t_0)$ and $\theta_S(t_0)$.

Physical model: Earth and Mars orbit the Sun with constant angular velocity on (approximately) circular orbits.

Observation: Initial angles of Mars and the Sun as seen from Earth: $o = (\theta_M(t_0), \theta_S(t_0))$, randomly chosen from a set of weekly (simulated) observations within Copernicus' lifetime (3665 observations in total).

Question: Implicit.

Correct answer: Time series $\big[a(t_1), \ldots, a(t_n)\big] = \big[(\theta_M(t_1), \theta_S(t_1)), \ldots, (\theta_M(t_n), \theta_S(t_n))\big]$ of $n = 20$ (later in training: $n = 50$) observations, with time steps $t_{i+1} - t_i$ of one week.

Implementation: Network depicted in Figure 5 with two latent neurons.

Key findings:

- *SciNet* predicts the angles of Mars and the Sun with a root mean square error below 0.4% (with respect to 2π).
- *SciNet* stores the angles ϕ_E and ϕ_M of the Earth and Mars as seen from the Sun in the two latent neurons (see Figure 6b) — that is, it recovers the heliocentric model of the solar system.

since this allows us to give the number of parameters stored in the latent representation a well defined meaning in terms of a dimension (see Appendix C).

Property 2 means that knowing some variables in the latent representation does not provide any information about any other latent variables; note that this depends on the distribution of the observations O.

We define a *minimal uncorrelated representation* R as an uncorrelated (sufficient) representation with a minimal number of parameters $|R|$. This formalizes what we consider to be a "simple" representation of physical data.

Without the assumption that the decoder is smooth, it would, in principle, always be sufficient to have a single latent variable, since a real number can store an infinite amount of information. Hence, methods from information theory, like the information bottleneck [24–26], are not the right tool to give the number of variables a formal meaning. In Appendix C, we use methods from differential geometry to show that the number of variables $|R|$ in a minimal (sufficient) representation corresponds to the number of relevant degrees of freedom in the observation data required to answer all possible questions.

4 Discussion

4.1 Comparison with previous work

Neural networks have become a standard tool to tackle problems where we want to make predictions without following a particular algorithm or imposing structure on the available data (see for example [27–29]) and they have been applied to a wide variety of problems in physics. For example, in condensed matter physics and generally in many-body settings, neural networks have proven particularly useful to characterize phase transitions [4–9]. In quantum optics, neural networks have been used to generate new experimental setups [10]. The above works focus on the prediction accuracy of neural networks, and do not extract information on what the network learned during training.

Closer to our work, neural networks have also been used to efficiently represent wave functions of specific quantum systems [30–40]. In particular, in [31], variational autoencoders are used to approximate the distribution of the measurement outcomes of a specific quantum state for a fixed measurement basis and the size of the neural network can provide an estimate for the complexity of the state. In contrast, our network can be used to produce representations of arbitrary states of simple systems without retraining. This allows us to extract information about the degrees of free-

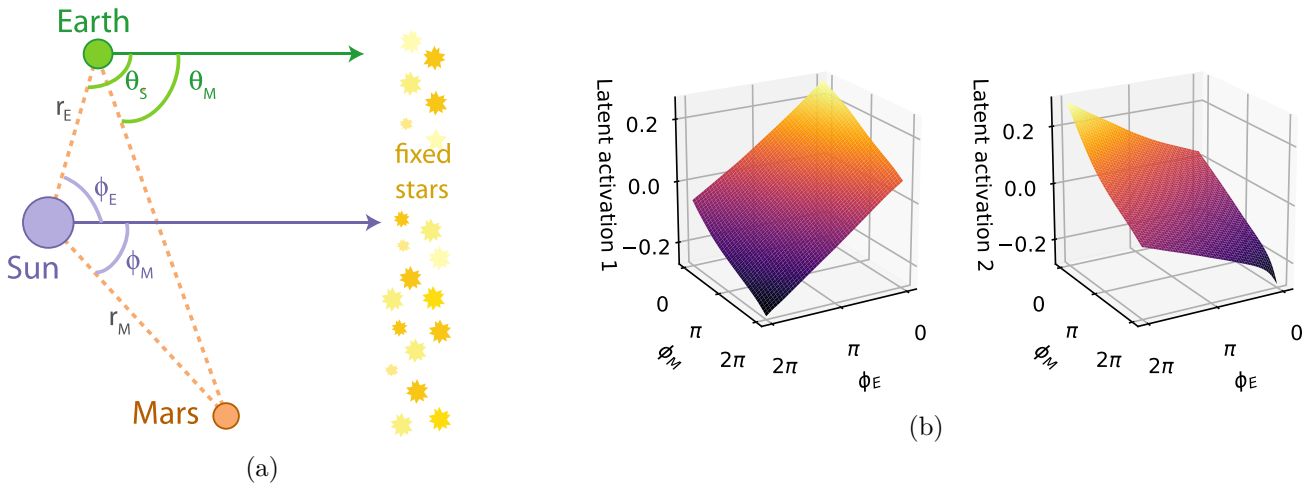

Figure 6: **Heliocentric model of the solar system.** *SciNet* is given the angles θ_S and θ_M of the Sun and Mars as seen from Earth at an initial time t_0 and has to predict these angles for later times. **(a) Physical setting.** The heliocentric angles ϕ_E and ϕ_M of the Earth and Mars are observed from the Sun; the angles θ_S and θ_M of the Sun and Mars are observed from Earth. All angles are measured relative to the fixed star background. **(b) Representation learned by *SciNet*.** The activation $r(t_0)$ of the two latent neurons at time t_0 (see Figure 5) is plotted as a function of the heliocentric angles ϕ_E and ϕ_M. The plots show that the network stores and evolves parameters that are linear combinations of the heliocentric angles, even though it was given the angles as observed from Earth. The slight non-linearity in the plots for extremal values of ϕ_M and ϕ_E is due to the sparsity of training data for these values.

dom required to represent any state of a (small) quantum system.

Another step towards extracting physical knowledge in an unsupervised way is presented in [13]. The authors show how the relevant degrees of freedom of a system in classical statistical mechanics can be extracted under the assumption that the input is drawn from a Boltzmann distribution. They make use of information theory to guide the unsupervised training of restricted Boltzmann machines, a class of probabilistic neural networks, to approximate probability distributions. While the focus in [13] is on systems for which the renormalization group procedure is applicable, here we presented a network architecture that is supposed to work, in principle, for arbitrary physical setups.

A different line of work has focused on using neural networks and other algorithmic techniques to better understand how humans are able gain an intuitive understanding of physics [41–43]. For example, it has been shown that neural networks can build up some physical intuition: given a picture of a tower built with blocks, they can predict with good accuracy if the tower is stable or will fall [44].

4.2 Future work

In general, the interpretability of the latent variables remains challenging. In our examples, the interpretation of the latent representation was aided by comparing it to known representations in physics. However, in general we might be interested in settings without a hypothesized representation that the network's learned representation can be compared to. In that case, one could, for example, try to apply methods from symbolic regression (see for example [45, 46]) to the trained encoder and decoder separately to obtain an analytic expression that might be more easily interpreted. Alternatively, one could try to develop more efficient methods that explicitly use the structure of the neural network.

4.3 Conclusion

In a recent overview of challenges for artificial intelligence in the near future [47], Lake *et al.* wrote:

> For deep networks trained on physics-related data, it remains to be seen whether higher layers will encode objects, general physical properties, forces and approximately Newtonian dynamics.

In this work, we have shown that neural networks can be used to recover physical variables

from experimental data. To do so, we have introduced a new network structure, *SciNet*, and employed techniques from unsupervised representation learning to encourage the network to find a minimal uncorrelated representation of experimental data.

The architecture of *SciNet* allows us to ask different questions about the physical system that the network has to answer using only its learned representation. Thus, the representation does not have to contain all information of the input data, but only the minimum amount of information that is necessary for the network to reply to all questions in some fixed set of questions.

In the case of our examples, the representations turned out to be the ones commonly used in physics textbooks. Our results therefore suggest that neural networks can indeed capture physical concepts and provide a step towards solving the problem posed by Lake *et al.*

Furthermore, the analogy between the process of reasoning of a physicist and representation learning provides insight about ways to formalize physical reasoning without adding prior knowledge about the system.

Source code and implementation details

The source code, details of the network structure and training process (as well as pre-trained *SciNets*) are available at `https://github.com/eth-nn-physics/nn_physical_concepts`. The networks were implemented using the Tensorflow library [48]. For all examples, the training process only takes a few hours on a standard laptop.

Acknowledgements

We would like to thank Alessandro Achille, Serguei Beloussov, Thomas Frerix, Viktor Gal, Thomas Häner, Maciej Koch-Janusz, Aurelien Lucchi, Andrea Rocchetto, Ying Zhe Ernest Tan, Jinzhao Wang and Leonard Wossnig for helpful discussions. We acknowledge support from the Swiss National Science Foundation through SNSF project No. 200020_165843 and through the National Centre of Competence in Research *Quantum Science and Technology* (QSIT). RR and LdR furthermore acknowledge support from the FQXi grant *Physics of the observer*.

Appendix

A Neural networks

For a detailed introduction to artificial neural networks and deep learning, see for example [27]. Here we give a very short overview of the basics.

Single artificial neuron. The building blocks of neural networks are single neurons (depicted in Figure 7). We can think of a neuron as taking several real inputs $x_1, \ldots, x_n$ and providing an output $\sigma(\sum_i w_i x_i + b)$, where the weights $w_i \in \mathbb{R}$ and the bias $b \in \mathbb{R}$ are tunable parameters and $\sigma : \mathbb{R} \to \mathbb{R}$ is called *activation function*. There are different possible choices for the activation function. For the implementation of the examples in Section 2, we use the exponential linear unit (ELU) [49]. The ELU is defined as follows for a hyper parameter $\alpha > 0$

$$\sigma_{\mathrm{ELU}}(z) = \begin{cases} z & \text{for } z > 0\,, \\ \alpha\,(e^z - 1) & \text{for } z \leq 0\,. \end{cases}$$

Neural network. A (feed-forward) neural network is created by arranging neurons in layers and forwarding the outcomes of the neurons in the i-th layer to neurons in the $(i+1)$-th layer (see Figure 9). The network as a whole can be viewed as a function $F : \mathbb{R}^n \to \mathbb{R}^m$ with $x_1, \ldots, x_n$ corresponding to the activations of the neurons in the first layer (which is called *input layer*). The activations of the input layer form the input for the second layer, which is a *hidden layer* (since it is neither an input nor an output layer). In the case of a fully connected network, each neuron in the $(i+1)$-th layer receives the activations of all neurons in the i-th layer as input. The activations of the m neurons in the last layer, which is called *output layer*, are then interpreted as the output of the function F.

It can be shown that neural networks are universal in the sense that any continuous function can be approximated arbitrarily well by a feedforward network with just one hidden layer by using sufficiently many hidden neurons. For a mathematical statement of the theorem, see [50, 51]. A visualization is given in [27].

Training. The weights and the biases of the neural network are not tuned by hand; instead, they are optimized using training samples, i.e.,

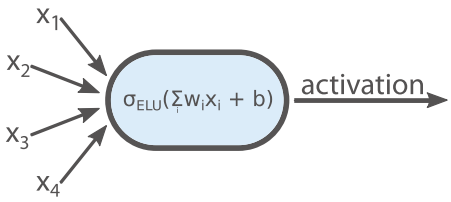

Figure 7: Single artificial neuron with weights w_i, bias b and ELU activation function σ_{ELU}. The inputs to the neuron are denoted by $x_1, \ldots, x_4$.

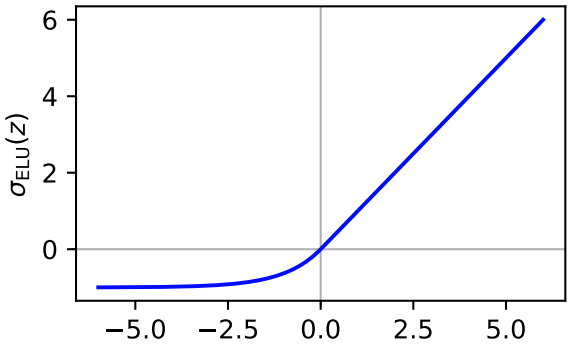

Figure 8: ELU activation function for $\alpha = 1$.

known input-output-pairs $(x, F^\star(x))$ of the function $F^\star$ that we would like to approximate. We may think of a neural network as a class of functions F_θ, where θ contains all the weights and biases of the network. A cost function $C\,(x, \theta)$ measures how close the output $F_\theta(x)$ of the network is to the desired output $F^\star(x)$ for an input x. For example, a common choice for the cost function is $C\,(x, \theta) = \|F^\star(x) - F_\theta(x)\|_2^2$.

To update the parameters θ, the gradient $\vec{\nabla}_\theta C\,(x, \theta)$ is computed and averaged over all training samples x. Subsequently, θ is updated in the negative gradient direction — hence the name *g*radient descent. In practice, the average of the gradient over all training samples is often replaced by an average over a smaller subset of training samples called a *mini-batch*; then, the algorithm is called *s*tochastic gradient descent. The backpropagation algorithm is used to perform a gradient descent step efficiently (see [27] for details).

B Variational autoencoders

The implementation of *SciNet* uses a modified version of so-called variational autoencoders (VAEs) [14, 18]. The standard VAE architecture does not include the question input used by *SciNet* and tries to reconstruct the input from the representation instead of answering a question. VAEs are one particular architecture used in the field of representation learning [16]. Here, we give a short overview over the goals of representation learning and the details of VAEs.

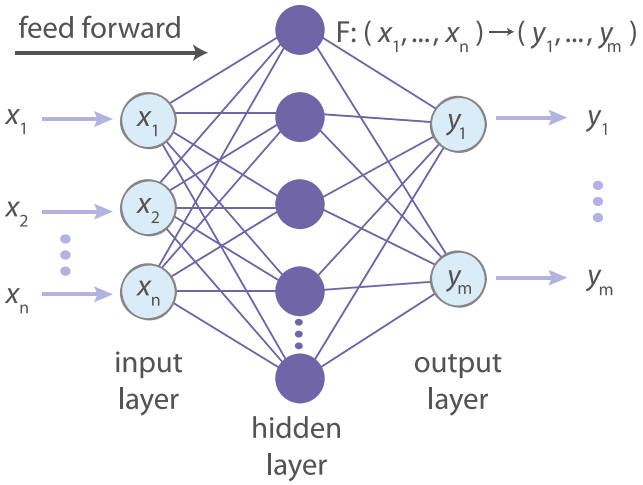

Figure 9: Fully connected (feed-forward) neural network with 3 layers. The network as a whole can be thought of as a function mapping the inputs $(x_1, \ldots, x_n)$ to the output $(y_1, \ldots, y_m)$.

Representation learning. The goal in representation learning is to map a higher-dimensional input vector x to a lower-dimensional representation z, commonly called the *latent vector*.[5] The representation z should still contain all the relevant information about x. In the case of an autoencoder, z is used to reconstruct the input x. This is motivated by the idea that the better the (low-dimensional) representation is, the better the input can be recovered from it.

Specifically, an autoencoder uses a neural network (*encoder*) to map the input x to a small number of latent neurons z. Then, another neural network (*decoder*) is used to reconstruct the input. During training, the encoder and decoder are optimized to maximize the reconstruction accuracy.

Probabilistic encoder and decoder. Instead of considering maps $x \mapsto z$ and $z \mapsto x$, we generalize to conditional probability distributions $p(z|x)$ for the encoder and $p(x|z)$ for the decoder. This is motivated by the Bayesian view that the most informative statement the encoder can make is to

[5] The variables x and z correspond to the observation o and the representation r used in the main text.

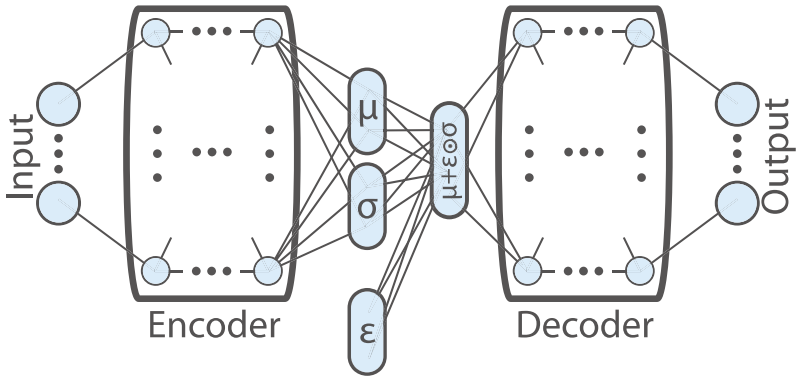

Figure 10: Network structure for a variational autoencoder. The encoder and decoder are described by conditional probability distributions $p(z|x)$ and $p(x|z)$ respectively. The output distribution of the encoder are the parameters μ_i and $\log(\sigma_i)$ for independent Gaussian distributions $z_i \sim \mathcal{N}(\mu_i, \sigma_i)$ of the latent variables. The reparameterization trick is used to sample from the latent distribution.

give a probability distribution over all latent vectors instead of outputting a single estimate. The same reasoning holds also for the decoder. We assume that $p(z|x)$ and $p(x|z)$ are members of parametric families $p_\phi(z|x)$ and $p_\theta(x|z)$, respectively.

In the simplest case, the optimal settings for ϕ and θ are learned as follows (see Figure 10 for a schematic of the network structure):

1. The encoder with parameters ϕ maps an input x to $p_\phi(z|x)$. In practice, the weights and biases of the encoder constitute the parameters ϕ. It is common to assume that the encoder distributions $p_\phi(z_i|x)$ are independent normal distributions $\mathcal{N}(\mu_i, \sigma_i)$; then, the encoder maps x to specific values of the vectors μ and σ (with components μ_i and σ_i, respectively).

2. A latent vector z is sampled from $p_\phi(z|x)$.

3. The decoder with parameters (weights and biases) θ maps the latent vector z to $p_\theta(x|z)$.

4. The parameters ϕ and θ are updated to maximize the likelihood of the original input x under the decoder distribution $p_\theta(x|z)$.

Reparameterization trick. The operation that samples a latent vector z from $p_\phi(z|x)$ is not differentiable with respect to the parameters ϕ and θ of the network. However, differentiability is necessary to train the network using stochastic gradient descent. This issue is solved by the reparameterization trick introduced in [14]: if $p_\phi(z_i|x)$ is a Gaussian with mean μ_i and standard deviation σ_i, we can replace the sampling operation using an auxiliary random number $\varepsilon_i \sim \mathcal{N}(0, 1)$. Then, a sample of the latent variable $z_i \sim \mathcal{N}(\mu_i, \sigma_i)$ can be generated by $z_i = \mu_i + \sigma_i \varepsilon_i$. Sampling ε_i does not interfere with gradient descent because, unlike $z_i \sim p_\phi(z_i|x)$, ε_i is independent of the trainable parameters ϕ and θ. Alternatively, one can view this way of sampling as injecting noise into the latent layer [19].

β-VAE cost function. A computationally tractable cost function for optimizing the parameters ϕ and θ was derived in [14]. This cost function was extended in [18] to encourage independency of the latent variables (or to encourage "disentangled" representations in the language of representation learning). The cost function in [18] is known as the β-VAE cost function and is given by

$$C_\beta = -\mathbb{E}_{z\sim p_\phi(z|x)} \left[\log p_\theta(x|z)\right] + \beta D_{\mathrm{KL}} \left[p_\phi(z|x) \| h(z)\right] .$$

The distribution $h(z)$ is a prior over the latent variables and is typically chosen as the unit Gaussian.[6] The first term can be viewed as the negative reconstruction loss, motivating the network to reconstruct the input data with high accuracy. The expectation value w.r.t. z is often estimated with a single sample, which works well if the minibatches are chosen sufficiently large [14]. The second term can be interpreted as a regularizer [14]. It uses the KL divergence, which can be thought

[6] The interpretation of $h(z)$ as a prior is obvious only when deriving VAEs as generative networks. For details, see [14].

of as a distance measure between probability distributions. Therefore, this term forces the distribution $p_\phi(z|x)$ to match the prior $h(z)$. Choosing a large hyper-parameter β limits the capacity of the latent representation z and motivates the network to learn an efficient representation. In [18], it was empirically shown that a large value for β also promotes disentangling of the latent variables. A theoretical motivation based on the information bottleneck can be found in [19].

To derive an explicit form of C_β, we again assume that $p_\phi(z|x) = \mathcal{N}(\mu, \sigma)$ with a diagonal covariance matrix $\sigma = \mathrm{diag}(\sigma_1, \ldots, \sigma_n)$. In addition, we make the common assumption that the decoder output $p_\theta(x|z)$ is a multivariate Gaussian with mean $\hat{x}$ and fixed covariance matrix $\hat{\sigma} = \frac{1}{\sqrt{2}}\mathbb{1}$. With these assumptions, the β-VAE cost function can be explicitly written as

$$C_\beta = \|\hat{x} - x\|_2^2 - \frac{\beta}{2}\left(\sum_i \log(\sigma_i^2) - \mu_i^2 - \sigma_i^2\right) + C\,.$$

The constant terms C do not contribute to the gradients used for training and can therefore be ignored.

C Interpretation of the number of latent variables

In Section 3, we require that the latent representation should contain a minimal amount of latent variables. However, it remains (formally) unclear how this relates to the structure of the given data. Proposition 2 below asserts that the minimal number of latent neurons corresponds to the relevant degrees of freedom in the observation data (in the sense described in Definition 1) required to answer all the questions that may be asked.

For simplicity, we describe the data with sets instead of random variables here. Note that the probabilistic structure was only used for Property 2 in Section 3, whereas here, we are only interested in the number of latent neurons and not in that they are mutually independent. We therefore consider the triple $(\mathcal{O}, \mathcal{Q}, a_{\mathrm{cor}})$, where $\mathcal{O}$ and $\mathcal{Q}$ are the sets containing the observation data and the questions respectively, and the function $a_{\mathrm{cor}} : (o, q) \mapsto a$ sends an observation $o \in \mathcal{O}$ and a question $q \in \mathcal{Q}$ to the correct reply $a \in \mathcal{A}$.

The following definition formalizes the number of degrees of freedom in (real-valued) data described by a triple $(\mathcal{O}, \mathcal{Q}, a_{\mathrm{cor}})$.

Definition 1. *We say that data described by a triple $(\mathcal{O} \subset \mathbb{R}^r, \mathcal{Q} \subset \mathbb{R}^s, a_{\mathrm{cor}} : \mathcal{O} \times \mathcal{Q} \to \mathcal{A} \subset \mathbb{R}^t)$ has dimension at least n if there exists an n-dimensional submanifold $\tilde{\mathcal{O}} \subset \mathcal{O} \subset \mathbb{R}^r$ and $k \in \mathbb{N}$ questions $q_1, \ldots, q_k$ such that $f : o \in \tilde{\mathcal{O}} \mapsto [a_{\mathrm{cor}}(o, q_1), \ldots, a_{\mathrm{cor}}(o, q_k)]$ is a diffeomorphism (considered as function $f : \tilde{\mathcal{O}} \to f(\tilde{\mathcal{O}})$).*

Less formally, the triple $(\mathcal{O}, \mathcal{Q}, a_{\mathrm{cor}})$ has dimension at least n, if there are questions that are able to capture n degrees of freedom from the observation data. Note that the smoothness is a natural requirement in the sense that we expect the dependence of the answer to the questions on the observational data to be robust.

Proposition 2 (Minimal representation for *SciNet*)**.** *A (sufficient) latent representation for data described by a triple $(\mathcal{O} \subset \mathbb{R}^r, \mathcal{Q} \subset \mathbb{R}^s, a_{\mathrm{cor}} : \mathcal{O} \times \mathcal{Q} \to \mathcal{A} \subset \mathbb{R}^t)$ of dimension at least n requires at least n latent variables.*

Proof. By definition, there exists an n-dimensional submanifold $\tilde{\mathcal{O}} \subset \mathcal{O}$ and k questions $q_1, \ldots, q_k$ such that $f : o \in \tilde{\mathcal{O}} \mapsto [a_{\mathrm{cor}}(o, q_1), \ldots, a_{\mathrm{cor}}(o, q_k)] \in \mathcal{I}$ is a diffeomorphism, i.e., where $\mathcal{I} := f(\tilde{\mathcal{O}})$ denotes the image of f. By contradiction, let us assume that there exists a (sufficient) representation described by an encoder $E : \mathcal{O} \to \mathcal{R} \subset \mathbb{R}^m$ with $m < n$ variables. By sufficiency of the representation, there exists a smooth decoder $D : \mathcal{R} \times \mathcal{Q} \to \mathcal{A}$ such that $D(E(o), q) = a_{\mathrm{cor}}(o, q)$ for all observations $o \in \mathcal{O}$ and questions $q \in \mathcal{Q}$. We define the smooth map $\tilde{D} : \mathcal{R} \to \mathbb{R}^{k \times t}$ by $\tilde{D}(r) = [D(r, q_1), \ldots, D(r, q_k)]$ and the preimage $\tilde{\mathcal{R}} := \tilde{D}^{-1}(\mathcal{I})$. By sufficiency of the representation, the restriction of the map $\tilde{D}$ to $\tilde{\mathcal{R}}$ denoted by $\tilde{D}|_{\tilde{\mathcal{R}}} : \tilde{\mathcal{R}} \to \mathcal{I}$ is a smooth and surjective map. However, by Sard's theorem (see for example [52]), the image $\tilde{D}(\tilde{\mathcal{R}})$ is of measure zero in $\mathcal{I}$ since the dimension of the domain $\tilde{\mathcal{R}} \subset \mathbb{R}^m$ is at most m, which is smaller than the dimension n of the image $\mathcal{I}$. This contradicts the surjectivity of $\tilde{D}|_{\tilde{\mathcal{R}}}$ and finishes the proof. □

We can consider an autoencoder as a special case of *SciNet*, where we ask always the same question and expect the network to reproduce the observation input. Hence, an autoencoder can be described by a triple $(\mathcal{O}, \mathcal{Q} = \{0\}, a_{\mathrm{cor}} : (o, 0) \mapsto o)$. As a corollary of Proposition 2, we show that in the case of an autoencoder, the required number of latent variables corresponds to the "relevant" number of generating factors of the data. The

following definition formalizes the notion of "relevance" for generating factors.

Definition 3. *We call a smooth function $H : \mathcal{G} \subset \mathbb{R}^d \to \mathbb{R}^r$ nondegenerate, if there exists an open subset $\mathcal{N} \subset \mathcal{G}$ in $\mathbb{R}^d$ such that the restriction of H on the open subset $H|_{\mathcal{N}} : \mathcal{N} \to H(\mathcal{N})$ is a diffeomorphism.*

Corollary 4 (Minimal representation for an autoencoder)**.** *Let $H : \mathcal{G} \subset \mathbb{R}^d \to \mathcal{O} \subset \mathbb{R}^r$ be a smooth, nondegenerate and surjective (data generating) function, and let us assume that $\mathcal{G}$ is bounded. Then the minimal sufficient representation for data described by a triple $(\mathcal{O}, \mathcal{Q} = \{0\}, a_{\text{cor}} : (o, 0) \mapsto o)$ contains d latent variables.*

Proof. First, we show the existence of a sufficient representation with d latent variables. We define the encoder mapping (and hence the representation) by $E : o \mapsto \text{argmin}[H^{-1}(\{o\})] \in \mathcal{G}$, where the minimum takes into account only the first vector entry.[7] We set the decoder equal to the smooth map H. By noting that $D(E(o), 0) = o$, this shows that d latent variables are sufficient.

Let us now show that there cannot exist a representation with less than d variables. By definition of a nondegenerate function H, there exists an open subset $\mathcal{N} \subset \mathcal{G}$ in $\mathbb{R}^d$ such that $H|_{\mathcal{N}} : \mathcal{N} \to H(\mathcal{N})$ is a diffeomorphism. We define the function $f : o \in H(\mathcal{N}) \mapsto a_{\text{cor}}(o, 0) \in \mathcal{I}$, where $\mathcal{I} = H(\mathcal{N})$. Since f is the identity map and hence a diffeomorphism, the data described by the triple $(\mathcal{O}, \mathcal{Q} = \{0\}, a_{\text{cor}} : (o, 0) \mapsto o)$ has dimension at least d. By Proposition 2, we conclude that at least d latent variables are required. □

D Cyclic representations

In this appendix, we explain the difficulty of a neural network to learn representations of cyclic parameters, which was alluded to in the context of the qubit example (Section 2.3, see [53, 54] for a detailed discussion relevant to computer vision). In general, this problem occurs if the data $\mathcal{O}$ that we would like to represent forms a closed manifold (i.e., a compact manifold without boundary), such as a circle, a sphere or a Klein bottle. In that case, several charts are required to describe this manifold.

As an example, let us consider data points lying on the unit sphere $\mathcal{O} = \{(x, y, z) : x^2 + y^2 + z^2 = 1\}$, which we would like to encode into a simple representation. The data can be (globally) parameterized with spherical coordinates $\phi \in [0, 2\pi)$ and $\theta \in [0, \pi]$ where $(x, y, z) = f(\theta, \phi) := (\sin\theta\cos\phi, \sin\theta\sin\phi, \cos\theta)$.[8] We would like the encoder to perform the mapping f^{-1}, where we define $f^{-1}((0, 0, 1)) = (0, 0)$ and $f^{-1}((0, 0, -1)) = (\pi, 0)$ for convenience. This mapping is not continuous at points on the sphere with $\phi = 0$ for $\theta \in (0, \pi)$. Therefore, using a neural network as an encoder leads to problems, as neural networks can only implement continuous functions. In practice, the network is forced to approximate the discontinuity in the encoder by a very steep continuous function, which leads to a high error for points close to the discontinuity.

In the qubit example, the same problem appears. To parameterize a qubit state ψ with two parameters, the Bloch sphere with parameters $\theta \in [0, \pi]$ and $\phi \in [0, 2\pi)$ is used: the state ψ can be written as $\psi(\theta, \phi) = (\cos(\theta/2), e^{i\phi}\sin(\theta/2))$ (see for example [55] for more details). Ideally, the encoder would perform the map $E : o(\psi(\theta, \phi)) := (|\langle\alpha_1, \psi(\theta, \phi)\rangle|^2, \ldots, |\langle\alpha_{N_1}, \psi(\theta, \phi)\rangle|^2) \mapsto (\theta, \phi)$ for some fixed binary projective measurements $\alpha_i \in \mathbb{C}^2$. However, such an encoder is not continuous. Indeed, assuming that the encoder is continuous, leads to the following contradiction:

$$\begin{aligned}(\theta, 0) &= E(o(\psi(\theta, \phi = 0))) \\ &= E(o(\lim_{\phi\to 2\pi} \psi(\theta, \phi))) \\ &= \lim_{\phi\to 2\pi} E(o(\psi(\theta, \phi))) \\ &= \lim_{\phi\to 2\pi} (\theta, \phi) = (\theta, 2\pi)\,,\end{aligned}$$

where we have used the periodicity of ϕ in the second equality and the fact that the Bloch sphere representation and the scalar product (and hence $o(\psi(\theta, \phi))$) as well as the encoder (by assumption) are continuous in ϕ in the third equality.

[7] Note that any element in $H^{-1}(\{o\})$ could be chosen.

[8] The function f is not a chart, since it is not injective and its domain is not open.

References

[1] Y. Aharonov and D. Rohrlich, *Quantum Paradoxes*, (Wiley-VCH, Weinheim, Germany, 2008).

[2] G. Chiribella and R. W. Spekkens (editors), *Quantum Theory: Informational Foundations and Foils*, Fundamental Theories of Physics Vol. 181 (Springer, Dordrecht, 2016).

[3] D. Frauchiger and R. Renner, "Single-world interpretations of quantum theory cannot be self-consistent", *Preprint* (2016), arXiv: 1604.07422.

[4] J. Carrasquilla and R. G. Melko, "Machine learning phases of matter", Nature Phys. 13, 431 (2017).

[5] E. P. L. v. Nieuwenburg, Y.-H. Liu, and S. D. Huber, "Learning phase transitions by confusion", Nature Phys. 13, 435 (2017).

[6] E. van Nieuwenburg, E. Bairey, and G. Refael, "Learning phase transitions from dynamics", *Preprint* (2017), arXiv: 1712.00450.

[7] P. Huembeli, A. Dauphin, P. Wittek, and C. Gogolin, "Automated discovery of characteristic features of phase transitions in many-body localization", *Preprint* (2018), arXiv: 1806.00419.

[8] G. Torlai and R. G. Melko, "Learning thermodynamics with Boltzmann machines", Phys. Rev. B 94, 165134 (2016).

[9] T. Ohtsuki and T. Ohtsuki, "Deep learning the quantum phase transitions in random electron systems: applications to three dimensions", J. Phys. Soc. Jpn. 86, 044708 (2017).

[10] A. A. Melnikov *et al.*, "Active learning machine learns to create new quantum experiments", Proc. Natl. Acad. Sciences 115, 1221 (2018).

[11] M. Schmidt and H. Lipson, "Distilling free-form natural laws from experimental data", Science 324, 81 (2009).

[12] M. Guzdial, B. Li, and M. O. Riedl, "Game Engine Learning from Video", Proc. Twenty-Sixth Int. Jt. Conf. on Artif. Intell. (2017).

[13] M. Koch-Janusz and Z. Ringel, "Mutual information, neural networks and the renormalization group", Nature Phys. 14, 578 (2018).

[14] D. P. Kingma and M. Welling, "Auto-Encoding Variational Bayes", *Preprint* (2013), arXiv: 1312.6114.

[15] G. E. Hinton and R. R. Salakhutdinov, "Reducing the dimensionality of data with neural networks", Science 313, 504 (2006).

[16] Y. Bengio, A. Courville, and P. Vincent, "Representation learning: a review and new perspectives", *Preprint* (2012), arXiv: 1206.5538.

[17] Y. Bengio, "Deep learning of representations: looking forward", *Preprint* (2013), arXiv: 1305.0445.

[18] I. Higgins *et al.*, "beta-VAE: learning basic visual concepts with a constrained variational framework", ICLR (2017).

[19] A. Achille and S. Soatto, "Information dropout: learning optimal representations through noisy computation", IEEE Transactions on Pattern Analysis Mach. Intell. 8828, 1 (2018).

[20] S. M. A. Eslami *et al.*, "Neural scene representation and rendering", Science 360, 1204 (2018).

[21] H. Kim and A. Mnih, "Disentangling by factorising", *Preprint* (2018), arXiv: 1802.05983.

[22] C. P. Burgess *et al.*, "Understanding disentangling in beta-VAE", NIPS (2018).

[23] M. Paris and J. Řeháček (editors), *Quantum State Estimation*, Lecture Notes in Physics (Springer, Berlin, Heidelberg, 2004).

[24] N. Tishby, F. C. Pereira, and W. Bialek, "The information bottleneck method", *Preprint* (2000), arXiv: 0004057.

[25] N. Tishby and N. Zaslavsky, "Deep learning and the information bottleneck principle", 2015 IEEE Inf. Theory Work. (ITW), 1 (2015).

[26] R. Shwartz-Ziv and N. Tishby, "Opening the black box of deep neural networks via information", *Preprint* (2017), arXiv: 1703.00810.

[27] M. A. Nielsen, Neural networks and deep learning, 2018, `http://neuralnetworksanddeeplearning.com/`.

[28] Y. LeCun, Y. Bengio, and G. Hinton, "Deep learning", Nature 521, 436 (2015).

[29] D. Silver *et al.*, "Mastering the game of Go with deep neural networks and tree search", Nature 529, 484 (2016).

[30] G. Carleo and M. Troyer, "Solving the quantum many-body problem with artificial neural networks", Science 355, 602 (2017).

[31] A. Rocchetto, E. Grant, S. Strelchuk, G. Carleo, and S. Severini, "Learning hard quantum

distributions with variational autoencoders", npj Quantum Inf. 4, 28 (2018).

[32] Z. Cai and J. Liu, "Approximating quantum many-body wave-functions using artificial neural networks", Phys. Rev. B 97 (2018).

[33] Y. Huang and J. E. Moore, "Neural network representation of tensor network and chiral states", *Preprint* (2017), arXiv: arXiv:1701.06246.

[34] D.-L. Deng, X. Li, and S. D. Sarma, "Machine learning topological states", Phys. Rev. B 96 (2017).

[35] M. Schmitt and M. Heyl, "Quantum dynamics in transverse-field Ising models from classical networks", SciPost Phys. 4 (2018).

[36] G. Torlai *et al.*, "Many-body quantum state tomography with neural networks", Nature Phys. 14, 447 (2018).

[37] Y. Nomura, A. S. Darmawan, Y. Yamaji, and M. Imada, "Restricted-Boltzmann-machine learning for solving strongly correlated quantum systems", Phys. Rev. B 96 (2017).

[38] D.-L. Deng, X. Li, and S. D. Sarma, "Quantum entanglement in neural network states", Phys. Rev. X 7 (2017).

[39] X. Gao and L.-M. Duan, "Efficient representation of quantum many-body states with deep neural networks", Nature Commun. 8 (2017).

[40] G. Torlai *et al.*, "Many-body quantum state tomography with neural networks", Nature Phys. 14, 447 (2018).

[41] M. B. Chang, T. Ullman, A. Torralba, and J. B. Tenenbaum, "A compositional object-based approach to learning physical dynamics", *Preprint* (2016), arXiv: 1612.00341.

[42] T. D. Ullman, A. Stuhlmüller, N. D. Goodman, and J. B. Tenenbaum, "Learning physical parameters from dynamic scenes", Cogn. Psychol. 104, 57 (2018).

[43] N. R. Bramley, T. Gerstenberg, J. B. Tenenbaum, and T. M. Gureckis, "Intuitive experimentation in the physical world", Cogn. Psychol. 105, 9 (2018).

[44] A. Lerer, S. Gross, and R. Fergus, "Learning physical intuition of block towers by example", *Preprint* (2016), arXiv: 1603.01312.

[45] J. R. Koza, "Genetic programming as a means for programming computers by natural selection", Stat. Comput. 4, 87 (1994).

[46] M. Quade, M. Abel, K. Shafi, R. K. Niven, and B. R. Noack, "Prediction of dynamical systems by symbolic regression", Phys. Rev. E 94, 012214 (2016).

[47] B. M. Lake, T. D. Ullman, J. B. Tenenbaum, and S. J. Gershman, "Building machines that learn and think like people", Behav. Brain Sciences 40 (2017).

[48] M. Abadi *et al.*, TensorFlow: Large-scale machine learning on heterogeneous systems, 2015, `https://www.tensorflow.org/`.

[49] D.-A. Clevert, T. Unterthiner, and S. Hochreiter, "Fast and accurate deep network learning by exponential linear units (ELUs)", *Preprint* (2015), arXiv: 1511.07289.

[50] G. Cybenko, "Approximation by superpositions of a sigmoidal function", Math. Control. Signals Syst. 2, 303 (1989).

[51] K. Hornik, M. Stinchcombe, and H. White, "Multilayer feedforward networks are universal approximators", Neural Networks 2, 359 (1989).

[52] J. Lee, *Introduction to Smooth Manifolds*, Graduate Texts in Mathematics, 2 ed. (Springer-Verlag, New York, 2012).

[53] N. Pitelis, C. Russell, and L. Agapito, "Learning a manifold as an atlas", IEEE Conf. on Comput. Vis. Pattern Recognit., 1642 (2013).

[54] E. O. Korman, "Autoencoding topology", *Preprint* (2018), arXiv: 1803.00156.

[55] M. A. Nielsen and I. L. Chuang, *Quantum Computation and Quantum Information: 10th Anniversary Edition*, (Cambridge University Press, 2010).